Journal of Systems Engineering and Electronics
Vol. 31, No. 4, August 2020, pp.826 – 840

Control allocation for a class of morphing aircraft with integer constraints based on Lévy flight

LU Yao[1,2,*], SUN You[1,2], LIU Xiaodong[1,2], and GAO Bo[1,2]

1. Beijing Aerospace Automatic Control Institute, Beijing 100854, China;
2. National Key Laboratory of Science and Technology on Aerospace Intelligence Control, Beijing 100854, China

Abstract: Aiming at tracking control of a class of innovative control effector (ICE) aircraft with distributed arrays of actuators, this paper proposes a control allocation scheme based on the Lévy flight. Different from the conventional aircraft control allocation problem, the particular characteristic of actuators makes the actuator control command totally subject to integer constraints. In order to tackle this problem, first, the control allocation problem is described as an integer programming problem with two desired objectives. Then considering the requirement of real-time, a metaheuristic algorithm based on the Lévy flight is introduced to tackling this problem. In order to improve the searching efficiency, several targeted and heuristic strategies including variable step length and inherited population initialization according to feedback and so on are designed. Moreover, to prevent the incertitude of the metaheuristic algorithm and ensure the flight stability, a guaranteed control strategy is designed. Finally, a time-varying simulation model is introduced to verifying the effectiveness of the proposed scheme. The contrastive simulation results indicate that the proposed scheme achieves superior tracking performance with appropriate actuator dynamics and computational time, and the improvements for efficiency are active and the parameter settings are reasonable.

Keywords: flight control, control allocation, optimization, Lévy flight, tracking control.

DOI: 10.23919/JSEE.2020.000056

1. Introduction

Many advanced aircraft utilize multiple and redundant effectors to tackle the requirements for control and fault tolerance capability. Thus, an appropriate control allocation scheme is necessary and important for such aircraft to map virtual control commands into actuator control commands. The general control allocation problems of over-actuated mechanical systems and flight control systems have been studied and summarized in plenty of studies [1 – 5]. To solve the problems, many optimization methods, such as the redistributed pseudo-inverse method, daisy chaining method, direct allocation method, simplex method, dynamic optimum-seeking method, linear programming (LP) and quadratic programming (QP) method, have been proposed. Most of the time, these methods are evaluated to be effective in solving the control allocation problems of the aircraft containing conventional effectors, such as rudders, ailerons and elevators.

The characteristic of deployed actuators plays an important role in achieving desired control commands. With the development of technology, many aircraft use heterogeneous actuators for superior stabilization and maneuver control. Different from the conventional effectors, the control models of some heterogeneous actuators, like reaction control system (RCS), are discontinuous. Deploying heterogeneous actuators, a class of morphing aircraft, called innovative control effector (ICE) aircraft, was first presented and investigated by Lockheed Martin Tactical Aircraft Systems [6]. The effectors of ICE aircraft are four distributed arrays each of which contains hundreds of shape-change actuators. There are only two states for each actuator, open or closed, i.e., each on/off-type actuator can merely supply either full or empty control effort (force and moment). The flight control system produces desired control efforts through allocating states of each actuator. Many studies [7 – 10] proposed control methods for the lateral-directional dynamics of ICE aircraft. In [7], an adaptive control method considering actuator failure was proposed and it achieved desired system performance. In [8], a fault-tolerant control allocation scheme was proposed and it could reject actuator faults and model uncertainties. In [9], a probabilistic robust controller was proposed for achieving the tracking control in the presence of uncertain actuator failures. In [10], an adaptive control scheme with control allocation through updating the number of operating actuators was proposed for ICE aircraft subject to uncertain time-varying uncertainties. Considering the large quantity of actuators, it is unrealistic to regard every actua-

Manuscript received May 05, 2019.
*Corresponding author.
This work was supported by the National Natural Science Foundation of China (61803357).

tor as a control variable. Therefore, in these studies the actuators are divided into four groups. This simplification of actuator model makes a certain difference between the mathematical model and the practical physical model and reduces the difficulty of getting actuator commands. Obviously, more meticulous division of actuators can make the actuator mathematical model closer to the practical physical model. However, more meticulous division of actuators will increase the number of control variables. Moreover, these studies assume that the active actuators within the same group have no differences in terms of generating force/moments. According to these assumptions, it can be found that each control variable must be an integer. This means the control allocation of actuators can be described as an integer programming problem.

The integer programming problem is usually an NP-hard problem. Some methods, such as the branch-bound method and the cutting plane method, are usually used to solve the precise optimum solution of the integer programming problem. However, the amount of computation of such conventional methods will quickly increase as the scale of problem expands, which will influence the real-time performance of the flight control system. Meanwhile, the design of the solving method is influenced by the form and number of constraints, which influences the universality of the method for different integer programming problems. Besides the polynomial algorithms and other exact methods, the metaheuristic algorithms have also been widely utilized to solve the integer programming problems in many engineering fields [11 – 15]. In [11], a genetic algorithm based heuristic method was designed for a hybrid system with manufacturing and remanufacturing. In [12], a variable neighborhood search metaheuristic algorithm was presented for the production routing problem. In [13], two different greedy heuristic methods including a population-based iterated greedy algorithm were proposed for the so-called weighted independent domination problem which is an NP-hard combinatorial optimization problem in graphs. In [14], the particle swarm optimization method was introduced to settling the problem of scheduling energy harvesting roadside units in vehicular ad-hoc networks. In [15], a novel simulated annealing algorithm embedding a mathematical model with an adjustment heuristic was developed for a parallel machine scheduling with time-dependent deterioration and multiple rate-modifying activities. According to the investigations from [16,17], sometimes the metaheuristic algorithms can achieve better solutions in comparison with the heuristic methods. The characteristic of the metaheuristic algorithm is that its amount of computation is mainly influenced by the parameter settings, such as the number of individuals, number of iterations and so on. Therefore, it is easy to control the computational time of algorithm via suitable parameter settings, which makes metaheuristic algorithms appropriate to those problems requiring strict real-time performance rather than a precise optimum solution.

Considering the advantages of metaheuristic algorithms and the strict real-time requirement of flight control, the studies [18,19] utilized a metaheuristic algorithm called cuckoo search algorithm (CSA) to solve the control allocation problem of ICE aircraft. In [18], the adaptive detection probability and amplification factor were designed to enhance the search capability of CSA. In [19], a heuristic population initialization method was designed to improve the quality of the initial population and the search efficiency. These two studies achieved certain effects but their schemes were lacking in the consideration of the contact between neighboring searches and the energy consumption of actuators. Moreover, the population initialization method in [19] and the creation of step length in [18] were not optimized enough. Therefore, further investigations that use metaheuristic algorithms to solve the control allocation problem of ICE aircraft are required.

In this paper, a control allocation scheme is proposed for improving the tracking performance of the flight control system of ICE aircraft. First, the lateral-directional dynamics of ICE aircraft is introduced and the control allocation problem is described as an optimization problem with integer constraints. Next, a scheme based on Lévy flight is proposed for tackling the problem and some components such as population initialization, step length with a form of feedback and so on are designed for efficiency. Following that, a guaranteed solution is designed to ensure the flight stability in case the quality of the searched solution is inferior. Then, the contrast simulations are carried out under a time-varying model of ICE aircraft and the results are discussed. Finally, some conclusions are drawn.

2. Problem formulation

2.1 System model description

The wing span of ICE aircraft [9] is illustrated in Fig. 1. There are four distributed effector arrays, the upper-surface leading-edge (ULE) array, lower-surface trailing-edge (LTE) array, upper-surface trailing-edge (UTE) array, and upper-surface wingtip (UTip) array, on each wing. There are totally 156 actuators on two wings, 78 on each wing. The four distributed arrays include 10, 22, 22 and 24 actuators, respectively. Each actuator can be turned “on” or “off” to generate full or no control effort.

The lateral-directional dynamics of ICE aircraft can be described as follows:

$$\dot{\boldsymbol{x}}(t) = \boldsymbol{A}(t)\boldsymbol{x}(t) + \boldsymbol{B}_v(t)\boldsymbol{v}(t) \tag{1}$$

where $\boldsymbol{x} = [V \quad p \quad r \quad \varphi]^{\mathrm{T}} \in \mathbf{R}^4$ represents the state vector; V, p, r and φ denote the body-axis lateral velocity, roll rate, yaw rate and roll angle, respectively. Assume that all state variables are measurable. $\boldsymbol{A}(t) \in \mathbf{R}^{4\times 4}$ and $\boldsymbol{B}_v(t) \in \mathbf{R}^{4\times 2}$ are the system matrices and their Frobenius norms are bounded and the system is controllable. $\boldsymbol{B}_v$ is the full column rank. $\boldsymbol{v}(t) = [v_1(t) \quad v_2(t)]^{\mathrm{T}} \in \mathbf{R}^2$ represents the ideal control input.

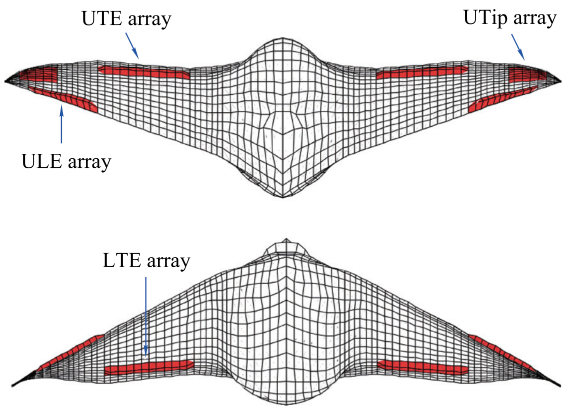

Fig. 1 Configuration of actuator arrays of ICE aircraft

The control objective is to make the system (1) track the following desired reference model:

$$\dot{\boldsymbol{x}}_m(t) = \boldsymbol{A}_m \boldsymbol{x}_m(t) + \boldsymbol{B}_m c(t) \tag{2}$$

where $\boldsymbol{A}_m \in \mathbf{R}^{4\times 4}$ and $\boldsymbol{B}_m \in \mathbf{R}^{4\times 1}$ are the predefined constant system matrix and vector of the reference, and $c(t)$ is the reference input signal. Let $\boldsymbol{e} = \boldsymbol{x} - \boldsymbol{x}_m$ represent the tracking error. Assume that the ideal control input $\boldsymbol{v}(t)$ can achieve the following target:

$$\dot{\boldsymbol{e}}(t) = \boldsymbol{A}_m \boldsymbol{e}(t). \tag{3}$$

This indicates the dynamics of tracking error is asymptotically stable, and the provided $\boldsymbol{A}_m$ is a Hurwitz matrix.

2.2 Control allocation problem

The ideal control input $\boldsymbol{v}(t)$ is achieved via the 156 actuators distributed on two wings. Drawing lessons from the assumptions in [9], all actuators are divided into eight groups and the following assumptions are made: (i) the control effects of the actuators that belong to the same group are equal; (ii) the actuators on the left wing generate negative control effort and those on the right wing generate positive control effort. The command of actuators is described by $\boldsymbol{n} = [n_1, \ldots, n_8]^{\mathrm{T}}$. According to the practical situation, n is constrained by the following sets:

$$\Omega_i = \{n_i | \underline{n}_i \leqslant n_i \leqslant \overline{n}_i, n_i \in \mathbf{Z}\}, \quad i = 1, 2, \ldots, 8 \tag{4}$$

where $\underline{n}_i \in \mathbf{Z}$ and $\overline{n}_i \in \mathbf{Z}$ represent the upper and lower boundary of n_i, respectively. It is obvious that $\boldsymbol{n}$ is an integer vector. The control model of actuators can be described as follows:

$$\boldsymbol{B}_u \boldsymbol{n}(t) = \overline{\boldsymbol{v}}(t), \quad n_i \in \Omega_i \tag{5}$$

where $\overline{\boldsymbol{v}}(t) \in \mathbf{R}^2$ represents the actual control input produced via the actuators, and $\boldsymbol{B}_u \in \mathbf{R}^{2\times 8}$ is the mapping matrix which is a full row rank.

Remark 1 Compared with [7 – 10,18,19], the actuators are divided into eight groups in this paper. This modeling is closer to the practical model and can enhance the control accuracy. However, this modeling also increases the number of control variables.

In terms of the above model, the control allocation problem of ICE aircraft can be described as obtaining appropriate actuator command $\boldsymbol{n}$ to ensure the tracking performance of the closed-loop system. Unfortunately, due to the integer constraints on $\boldsymbol{n}$, it is difficult to find a solving method from the existing literature investigating aircraft control allocation, and an error between the ideal control input $\boldsymbol{v}$ and actual control input $\overline{\boldsymbol{v}}$ almost always occurs. In [19], it was concluded that the tracking error of system was related to this error. Then the primary objective of the control allocation problem of ICE aircraft can be represented as the following optimization problem:

$$\min_{n_i \in \Omega_i} \|(\boldsymbol{v} - \boldsymbol{B}_u \boldsymbol{n})\|_2 \tag{6}$$

where $\|\cdot\|_2$ denotes 2-norm. In addition, another noteworthy objective is to minimize the wear and tear of actuators. In an optimization framework, this secondary objective can be reflected by adding a cost index into (6):

$$\min_{n_i \in \Omega_i} \left(\|(\boldsymbol{v} - \boldsymbol{B}_u \boldsymbol{n})\|_2 + \frac{\psi}{2} (\boldsymbol{n} - \boldsymbol{n}_p)^{\mathrm{T}} (\boldsymbol{n} - \boldsymbol{n}_p) \right) \tag{7}$$

where $\boldsymbol{n}_p$ is the preferred value of $\boldsymbol{n}$ and it is represented by the last actuator control command in this paper, and $\psi > 0$ is a coefficient to reflect the weight between the primary and secondary objectives.

Due to the numerous constraints, the convex quadratic integer programming problem (7) is difficult to be exactly solved within a strict time limit. To solve the optimization problem (7), in this paper, a metaheuristic algorithm with some heuristic ideas is proposed for searching the superior optimum solution $\boldsymbol{n}$. Then a cost function $J(\boldsymbol{v}, \boldsymbol{n}, \boldsymbol{n}_p)$ is formulated to assist the searching according to (7):

$$J = \|(\boldsymbol{v} - \boldsymbol{B}_u \boldsymbol{n})\|_2 + \frac{\psi}{2} (\boldsymbol{n} - \boldsymbol{n}_p)^{\mathrm{T}} (\boldsymbol{n} - \boldsymbol{n}_p), \quad n_i \in \Omega_i. \tag{8}$$

The value of the cost function will be called fitness value in later chapters.

3. Design of control allocation scheme

Generally, the searching process of a metaheuristic algorithm, the main components of which are the population scale, iteration, renewal manner of the individual and mutation factor, includes two phases: global search phase and local search phase. The strategies and parameter settings of the algorithm should be assorted with the characteristics of different phases.

3.1 Renewal manner of the individual

In this paper, the Lévy flight is introduced to updating the individuals. The Lévy flight process [20,21] which has already been identified in a number of animals and insects is a random walk in which the increments are distributed according to a heavy-tailed probability distribution. Some studies [22,23] verified that this process is an optimum search pattern for the case of "no preferred direction" and non-replenishable targets at unknown positions. As an important content, the Lévy flight is introduced to many metaheuristic algorithms and a typical representative of them is the CSA which has been applied to many engineering fields [24]. Let $\boldsymbol{n}_j^t$ denote the jth solution in the tth generation of the population. The new solution $\boldsymbol{n}_j^{t+1}$ updated via Lévy flight can be described as follows:

$$\boldsymbol{n}_j^{t+1} = \boldsymbol{n}_j^t + \mathrm{round}(\boldsymbol{\alpha} \otimes \boldsymbol{L}(\lambda)) \tag{9}$$

where $\boldsymbol{\alpha} \in \mathbf{R}^8$ represents the step length vector, $\otimes$ denotes Hadamard multiplication operator, $\mathrm{round}(\cdot)$ denotes the rounding operation, $\boldsymbol{L}(\lambda) = [l_1(\lambda), \dots, l_8(\lambda)]^{\mathrm{T}}$ is the random step length and $l_i(\lambda)$ follows the Lévy distribution [23]:

$$l_i(\lambda) \sim t^{-\lambda}, \quad 1 < \lambda \leqslant 3 \tag{10}$$

which has an infinite variance with an infinite mean. Here λ is a Lévy flight parameter which influences the magnitude of the random step length. Table 1 shows the statistic $|l(\lambda)|$ obtained via 10 000 random walks under different λ with the restriction $|l(\lambda)| \leqslant 50$.

Table 1 Statistics of $|l(\lambda)|$ under different λ

Statistics	$\lambda=1.8$	$\lambda=2$	$\lambda=2.3$	$\lambda=2.5$	$\lambda=2.8$
Number of random walks	10 000	10 000	10 000	10 000	10 000
Number of $\lvert l(\lambda)\rvert \leqslant 1$/Average of all $\lvert l(\lambda)\rvert \leqslant 1$	5 363/ 0.407 4	5 013/ 0.446 7	3 532/ 0.485 5	2 128/ 0.494 4	426/ 0.502 9
Number of $1 < \lvert l(\lambda)\rvert \leqslant 2.5$/ Average of all $1 < \lvert l(\lambda)\rvert \leqslant 2.5$	2 171/ 1.591 8	2 550/ 1.589 8	3 053/1.640 5	2 660/ 1.701 2	605/ 1.746 9
Number of $2.5 < \lvert l(\lambda)\rvert \leqslant 5$/Average of all $2.5 < \lvert l(\lambda)\rvert \leqslant 5$	1 048/ 3.527 7	1 113/ 3.467 3	1 791/ 3.489 2	2 502/ 3.590 8	942/ 3.708 4
Number of $5 < \lvert l(\lambda)\rvert \leqslant 10$/ Average of all $5 < \lvert l(\lambda)\rvert \leqslant 10$	591/ 7.062 2	630/6.983 3	935/ 6.799 3	1 664/ 6.938 4	1 737/ 7.417 2
Number of $\lvert l(\lambda)\rvert > 10$/Average of all $\lvert l(\lambda)\rvert > 10$	827/ 28.358	694/ 26.475	689/ 22.777	1 046/ 22.230	6 290/ 26.758
Average of all $\lvert l(\lambda)\rvert$	3.696 4	3.292 5	3.502 3	4.935 9	18.596

According to the statistics, assuming that the parameter $\boldsymbol{\alpha} = [1, \dots, 1]^{\mathrm{T}}$, the appropriate interval of the parameter λ is [2.3,2.8] in the global search which needs a larger random step length, and the appropriate interval of the parameter λ is [1.8,2.3) in the local search which needs a smaller random step length. The search mode is determined by the comparison between $J(\boldsymbol{v}, \boldsymbol{n}_j^t, \boldsymbol{n}_p)$ and a parameter η: if $J(\boldsymbol{v}, \boldsymbol{n}_j^t, \boldsymbol{n}_p) > \eta$, then the search mode is regarded as a global search and λ is chosen as λ_g; if $J(\boldsymbol{v}, \boldsymbol{n}_j^t, \boldsymbol{n}_p) \leqslant \eta$, then the search mode is regarded as a local search and λ is chosen as λ_l.

The design of parameters $\boldsymbol{\alpha}$ and λ should be coordinated with each other. The parameter $\boldsymbol{\alpha}$ influences the change of $\boldsymbol{n}_j^t$ to $\boldsymbol{n}_j^{t+1}$. It should be noticed that the influences on $\overline{\boldsymbol{v}}$ created by different actuator groups are different. Considering this, a feedback system is established for designing the parameter $\boldsymbol{\alpha}$. Let

$$\boldsymbol{\alpha} = [\alpha_1, \dots, \alpha_8]^{\mathrm{T}},$$

$$\boldsymbol{B}_u = [\boldsymbol{B}_1, \dots, \boldsymbol{B}_8] = \begin{bmatrix} b_{11} & \cdots & b_{18} \\ b_{21} & \cdots & b_{28} \end{bmatrix},$$

$$\Delta\boldsymbol{v} = \boldsymbol{v} - \boldsymbol{B}_u \boldsymbol{n}_j^t.$$

According to the comparison between $\boldsymbol{B}_i$ and $\Delta\boldsymbol{v}$, considering the above-mentioned magnitude of the random step length under different selections of λ, the following rule for α_i is established:

$$\alpha_i = \begin{cases} 0.01, \quad \|\boldsymbol{B}_i\|_2 \geqslant 5\|\Delta\boldsymbol{v}\|_2 \\ (\|\Delta\boldsymbol{v}\|_2/\|\boldsymbol{B}_i\|_2) - 0.1, \\ \qquad 2.5\|\Delta\boldsymbol{v}\|_2 \leqslant \|\boldsymbol{B}_i\|_2 < 5\|\Delta\boldsymbol{v}\|_2 \\ (\|\Delta\boldsymbol{v}\|_2/3\|\boldsymbol{B}_i\|_2) + 1/6, \\ \qquad \|\Delta\boldsymbol{v}\|_2 \leqslant \|\boldsymbol{B}_i\|_2 < 2.5\|\Delta\boldsymbol{v}\|_2 \\ (0.25\|\Delta\boldsymbol{v}\|_2/\|\boldsymbol{B}_i\|_2) + 0.25, \\ \qquad 0.2\|\Delta\boldsymbol{v}\|_2 \leqslant \|\boldsymbol{B}_i\|_2 < \|\Delta\boldsymbol{v}\|_2 \\ 0.1, \quad \|\boldsymbol{B}_i\|_2 < 0.2\|\Delta\boldsymbol{v}\|_2 \end{cases}. \tag{11}$$

Under this rule, the matching parameters λ_g and λ_l are chosen as $\lambda_g = 2.5$ and $\lambda_l = 2.0$, respectively. It should be noted that this rule is simple and eclectic. Obviously, the rule can be established more perfect via more meticulous analysis, like the branch-bound method or the cutting plane method. However, that will increase the computation load and take up more storage space of the onboard software. Therefore, a degree of trade-off is unavoidable.

Remark 2 Lu et al. [18] also designed an adaptive rule of the step length vector. Compared with the rule in [18], the rule (11) considers the mapping matrix $\boldsymbol{B}_u$, i.e., the possible control effect of each group. This is conducive to the search directions of individuals and improves the search efficiency.

3.2 Population initialization

A high-quality initial population is propitious to get a final superior solution. In [19], a population initialization method was proposed, but it is unstable as the problem scale expands and the energy wear of actuators is omitted. Therefore, an improved population initialization strategy needs to be designed.

Considering the secondary objective in (7), the last actuator control input $\boldsymbol{n}_p$ can be selected as a part of the current initial population because this can ensure that the second half of the cost function (8) is zero. Let σ denote the proportion of the number of $\boldsymbol{n}_p$ to the number of individuals in population, $\vartheta = J(\boldsymbol{v}(t-1), \boldsymbol{n}_p, \boldsymbol{n}_p(t-1))$ denote the fitness value of the best searched solution in the $(t-1)$th generation. Considering that $\boldsymbol{B}_u$ is constant, it can be inferred that if both $\|\boldsymbol{v}(t) - \boldsymbol{v}(t-1)\|_2$ and ϑ are small, $\boldsymbol{n}_p$ is probably a superior solution in the current period. Under this circumstance, the selected value of σ should be larger; contrarily, the selected value of σ should be smaller. Based on this, the parameter σ is designed as follows:

$$\sigma = \begin{cases} \min(0.5, 0.05/\|\boldsymbol{v}(t) - \boldsymbol{v}(t-1)\|_2), \\ \qquad \|\boldsymbol{v}(t) - \boldsymbol{v}(t-1)\|_2 \neq 0; t \neq 1 \text{ and } \vartheta \leqslant \overline{\vartheta} \\ 0.5, \quad \|\boldsymbol{v}(t) - \boldsymbol{v}(t-1)\|_2 = 0; t \neq 1 \text{ and } \vartheta \leqslant \overline{\vartheta} \\ 0, \quad t = 1 \text{ or } \vartheta > \overline{\vartheta} \end{cases} \tag{12}$$

where $\overline{\vartheta} > 0$ is a predetermined criterion. Let N represent the number of individuals of population; the final number of $\boldsymbol{n}_p$ in the initial population is $\mathrm{fix}(\sigma N)$ where $\mathrm{fix}(\cdot)$ denotes rounding the element to the nearest integer towards zero.

The other initial individuals the number of which is represented by M are created via the Tent map. The Tent map [25] which is related to Devaney chaos can stably create qualified individuals from the possible space according to the following formula:

$$\tau_{k+1}^i = \begin{cases} 2\tau_k^i, \quad 0 < \tau_k^i < 0.5 \\ \varsigma, \quad \tau_k^i = 0 \text{ or } \tau_k^i = 0.5 \text{ or } \tau_k^i = 1 \\ 2(1-\tau_k^i), \quad 0.5 < \tau_k^i < 1 \end{cases} \tag{13}$$

where ς denotes a random number within the interval of (0,1). When initializing population, a random qualified individual $\boldsymbol{n}$ is created and mapped into the interval of chaotic variables via $\tau_k^i = (n_i - \underline{n}_i)/(\overline{n}_i - \underline{n}_i)$. After this, $2M$ iterations are carried out via (13) and then reduce the chaotic sequence into the constraints (4) via $n_i = \underline{n}_i + (\overline{n}_i - \underline{n}_i) \cdot \tau_k^i$. Following that, calculate the fitness values of all $2M$ alternatives and select M superior individuals into the initial population. Then all the initial individuals are determined.

Remark 3 Compared with the population initialization method designed in [19], the proposed strategy considers the connection between the present ideal control input $\boldsymbol{v}(t)$ and the last ideal control input $\boldsymbol{v}(t-1)$, and then creates the initial population according to the quality of the last searched optimum individual. Moreover, all the initial individuals created via the proposed strategy must be within the constrained sets (4). However, the initial individuals created via the method in [19] are likely to go beyond the boundaries of the constrained sets.

3.3 Individual qualification

In the searching process, some generated individuals may escape the constraints (4). To tackle this problem, when a new individual $\boldsymbol{n}^* = [n_1^*, \dots, n_8^*]^{\mathrm{T}}$ is generated via (9), the following measure is adopted:

$$\widehat{n}_i^* = \begin{cases} \overline{n}_i, \quad n_i^* > \overline{n}_i \\ \underline{n}_i, \quad n_i^* < \underline{n}_i \\ n_i^*, \quad \text{others} \end{cases}. \tag{14}$$

Then the updated individual $\widehat{\boldsymbol{n}}^* = [\widehat{n}_1^*, \dots, \widehat{n}_8^*]^{\mathrm{T}}$ is fully qualified.

3.4 Other rules

Besides the above strategies, there are some other rules used to improve the searching efficiency. First, to avoid the algorithm falling into local optimum, a targeted rule similar to mutation operation is adopted: if the quality of one individual cannot be improved in five iterations, this individual will be abandoned and replaced with a new individual. Second, to save the searching time, the following rule is adopted: if the fitness value of one individual is smaller than the criterion parameter χ, then stop the searching process and employ this individual as the final searched optimum solution.

3.5 Guaranteed solution of the control allocation scheme

The general shortcoming of metaheuristic algorithms is that the performance of the final searched solution cannot be ensured, i.e., the quality of the final searched solution is unstable. For a flight control system, the stability of the closed-system must be absolutely ensured. Considering this, the following guaranteed solution is used:

$$\overline{\boldsymbol{\theta}} = \boldsymbol{B}_u^+ \boldsymbol{v}(t) \tag{15}$$

where $(\cdot)^+$ denotes pseudo-inverse. $\overline{\boldsymbol{\theta}}$ is a real-valued control effect vector and an exact solution because $\boldsymbol{B}_u$ is a full row rank matrix. Then the actual actuator commands can be obtained via rounding $\overline{\boldsymbol{\theta}}$. This is an obvious and natural approach which could be somewhat similar to the method in [7] and it could be straightforward to implement. Let $\boldsymbol{\theta} = \mathrm{round}(\overline{\boldsymbol{\theta}})$. Through appropriate design of the ideal control input $\boldsymbol{v}(t)$ and deployment of actuators, the control capability can be enough to ensure $\boldsymbol{\theta}$ meeting the constraints (4). Then add $\boldsymbol{\theta}$ into the initial population as the guaranteed solution.

According to the above-mentioned strategies, the control system for ICE aircraft can be illustrated in Fig. 2.

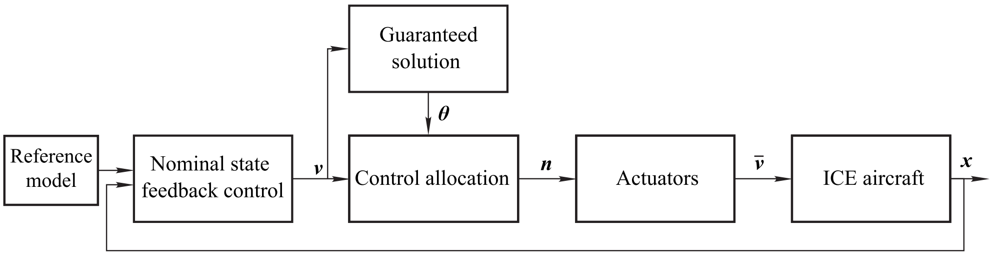

Fig. 2 Control system structure of ICE aircraft

3.6 Stability analysis

Generally, due to the constraints (6), an error almost always occurs between $\boldsymbol{v}(t)$ and $\overline{\boldsymbol{v}}(t)$. In terms of (3), it can be concluded that if $\boldsymbol{v}(t)$ acts on the system, there exists a global Lyapunov function $W = \boldsymbol{e}^{\mathrm{T}}\boldsymbol{P}\boldsymbol{e}$ in the closed-loop system making $\dot{W} = -\boldsymbol{e}^{\mathrm{T}}\boldsymbol{Q}\boldsymbol{e}$, where $\boldsymbol{P}$ is a constant positive definite symmetric matrix and $-\boldsymbol{Q} = -(\boldsymbol{A}_m^{\mathrm{T}}\boldsymbol{P}+\boldsymbol{P}\boldsymbol{A}_m)$ is a corresponding negative definite matrix. Let $\boldsymbol{\delta} = \boldsymbol{v}(t) - \overline{\boldsymbol{v}}(t)$. The dynamics of the tracking error $\boldsymbol{e}$ can be described as follows when $\overline{\boldsymbol{v}}(t)$ acts on the system:

$$\dot{\boldsymbol{e}} = \boldsymbol{A}_m(\boldsymbol{e} + \boldsymbol{A}_m^{-1}\boldsymbol{B}_v(t)\boldsymbol{\delta}). \tag{16}$$

Consider the alternate Lyapunov function $W = \boldsymbol{e}^{\mathrm{T}}\boldsymbol{P}\boldsymbol{e}$. In terms of (16) the time derivative of W can be written as

$$\dot{W} = -\boldsymbol{e}^{\mathrm{T}}\boldsymbol{Q}\boldsymbol{e} + 2\boldsymbol{\delta}^{\mathrm{T}}\boldsymbol{B}_v^{\mathrm{T}}\boldsymbol{P}\boldsymbol{e}. \tag{17}$$

Let $\boldsymbol{n}_{\mathrm{best}}$ represent the final searched solution. Because $\boldsymbol{\theta}$ is an individual in the initial population, and therefore $J(\boldsymbol{n}_{\mathrm{best}}) \leqslant J(\boldsymbol{\theta})$, i.e.,

$$\begin{aligned}\|\boldsymbol{\delta}\|_2 = \|(\boldsymbol{v} - \boldsymbol{B}_u\boldsymbol{n}_{\mathrm{best}})\|_2 \leqslant \|(\boldsymbol{v} - \boldsymbol{B}_u\boldsymbol{\theta})\|_2 + \\ \frac{\psi}{2}(\boldsymbol{\theta} - \boldsymbol{n}_p)^{\mathrm{T}}(\boldsymbol{\theta} - \boldsymbol{n}_p) - \\ \frac{\psi}{2}(\boldsymbol{n}_{\mathrm{best}} - \boldsymbol{n}_p)^{\mathrm{T}}(\boldsymbol{n}_{\mathrm{best}} - \boldsymbol{n}_p).\end{aligned} \tag{18}$$

Let $\Delta\boldsymbol{\theta} = \boldsymbol{\theta} - \overline{\boldsymbol{\theta}}$. Then the following inequality yields

$$\begin{aligned}\|(\boldsymbol{v} - \boldsymbol{B}_u\boldsymbol{\theta})\|_2 = \|(\boldsymbol{v} - \boldsymbol{B}_u\overline{\boldsymbol{\theta}} - \boldsymbol{B}_u\Delta\boldsymbol{\theta})\|_2 \leqslant \\ \|((\boldsymbol{I}^{2\times 2} - \boldsymbol{B}_u\boldsymbol{B}_u^{+})\boldsymbol{v} - \boldsymbol{B}_u\Delta\boldsymbol{\theta})\|_2.\end{aligned} \tag{19}$$

Notice that $\|\Delta\boldsymbol{\theta}\|_2 = \|\mathrm{round}(\overline{\boldsymbol{\theta}}) - \overline{\boldsymbol{\theta}}\|_2 \leqslant \sqrt{2}$, $\boldsymbol{v}(t)$ is bounded and $\boldsymbol{B}_u$ and $\boldsymbol{I}^{2\times 2} - \boldsymbol{B}_u\boldsymbol{B}_u^{+}$ are both fixed. Therefore, the term $\|(\boldsymbol{v} - \boldsymbol{B}_u\boldsymbol{\theta})\|_2$ is bounded. Moreover, considering the variables $\boldsymbol{\theta}, \boldsymbol{n}_{\mathrm{best}}$ and $\boldsymbol{n}_p$ are within the ranges in (14), the terms $\psi(\boldsymbol{\theta} - \boldsymbol{n}_p)^{\mathrm{T}}(\boldsymbol{\theta} - \boldsymbol{n}_p)/2$ and $\psi(\boldsymbol{n}_{\mathrm{best}} - \boldsymbol{n}_p)^{\mathrm{T}}(\boldsymbol{n}_{\mathrm{best}} - \boldsymbol{n}_p)/2$ in (18) are both bounded. These indicate that the error $\boldsymbol{\delta}(t)$ is bounded. Let $\overline{\delta}$ represent the upper boundary of $\|\boldsymbol{\delta}(t)\|_2$, $\overline{b}$ represent the upper boundary of $\|\boldsymbol{B}_v\|_F$ where $\|\cdot\|_F$ denotes the Frobenius norm of a matrix, $\overline{P}$ represent the upper boundary of $\|\boldsymbol{P}\|_F$, and $\lambda_Q > 0$ represent the minimum eigenvalue of $\boldsymbol{Q}$. Then from (17) we get

$$\begin{aligned}\dot{W} \leqslant -\lambda_Q\|\boldsymbol{e}\|_2^2 + 2\|\boldsymbol{\delta}\|_2\|\boldsymbol{B}_v\|_F\|\boldsymbol{P}\|_F\|\boldsymbol{e}\|_2 \leqslant \\ -\lambda_Q\|\boldsymbol{e}\|_2^2 + 2\overline{\delta}\,\overline{b}\,\overline{P}\|\boldsymbol{e}\|_2.\end{aligned} \tag{20}$$

It is not hard to see that when $\|\boldsymbol{e}\|_2 > 2\overline{\delta}\,\overline{b}\,\overline{P}/\lambda_Q, \dot{W} < 0$. This implies that the tracking error $\boldsymbol{e}$ is bounded.

3.7 Specific searching process

For an individual, its evolutionary process in one period can be illustrated in Fig. 3 where $t_{\max}$ represents the maximum of iterations. After all individuals are finished to be updated, the final searched optimum solution $\boldsymbol{n}_{\mathrm{best}}$ which has the best fitness value within the whole searching process is obtained. Then compare $\overline{J}(\boldsymbol{n}_{\mathrm{best}})$ with $\overline{J}(\boldsymbol{\theta})$ and the final actuator control command is determined.

3.8 Time complexity of algorithm

The time complexity of a metaheuristic algorithm is an important index reflecting the real-time performance of the algorithm. Especially for the control allocation of a flight vehicle which needs on-line calculations, it influences the practicality of the algorithm severely. Generally, the time complexity of a metaheuristic algorithm is evaluated via the number of the comparisons of the fitness values between two individuals, or the maximum number of iterations [26]. It can be described as $O(f(\sigma_1, \sigma_2, \ldots))$, where $f(\cdot)$ represents an auxiliary function, and $\sigma_1, \sigma_2, \ldots$ represent the factors influencing the computational time of the algorithm. Let N represent the number of individuals in population. Referring to Fig. 3, considering the possible most complex iterative process, there are four main factors influencing the computation time of the proposed algorithm as follows:

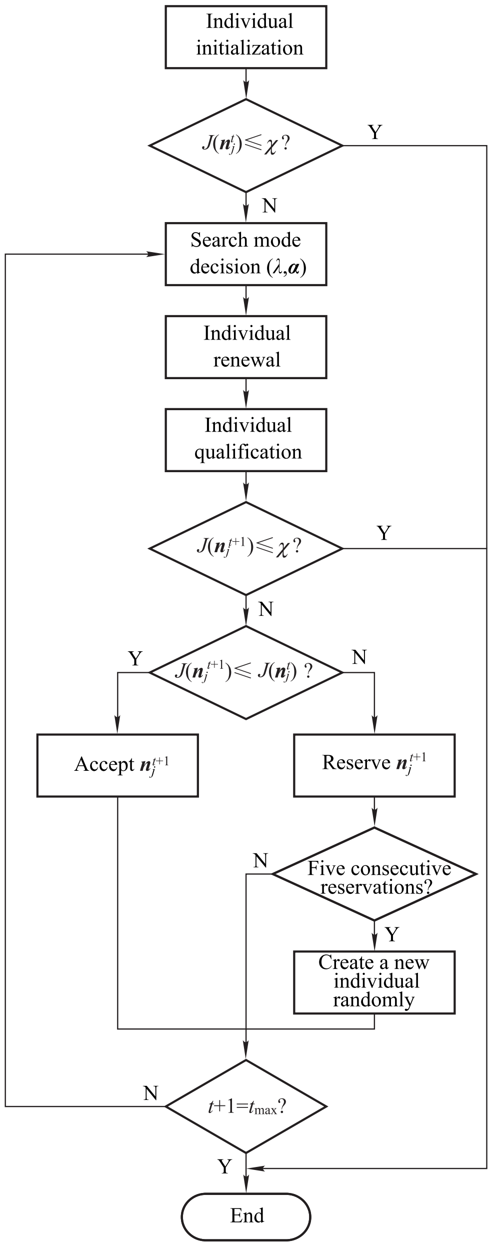

Fig. 3 Evolutionary process of an individual

(i) one comparison between ϑ and $\overline{\vartheta}$ from (12);

(ii) $2N$ iterations according to (13) for creating an original initial population and $N(N-1)/2$ comparisons for selecting the superior individuals and putting them into the final initial population;

(iii) $t_{\max}$ iterations and four comparisons (between $J(\boldsymbol{n}_j^t)$ and η, $J(\boldsymbol{n}_j^{t+1})$ and δ, $J(\boldsymbol{n}_j^{t+1})$ and $J(\boldsymbol{n}_j^t)$, holding times and five mentioned in other rules) in every iteration for each individual;

(iv) $t_{\max}$ comparisons between t and $t_{\max}$.

Thus, the time complexity of the proposed algorithm can be represented as $O((4N+1)t_{\max} + (N^2+3N)/2+1)$. This indicates that the computational time of the proposed algorithm can be controlled via choosing appropriate N and $t_{\max}$ with the considerations of the performance of the onboard processor.

4. Simulation results

In this section, the proposed control allocation scheme is applied to the lateral dynamic model of ICE aircraft to verify its performance. In order to reduce the difficulty of design of the ideal control law, the lateral-directional dynamics of ICE aircraft (1) are described as follows:

$$\dot{\boldsymbol{x}}(t) = (\overline{\boldsymbol{A}} + \Delta\overline{\boldsymbol{A}}(t))\boldsymbol{x}(t) + (\overline{\boldsymbol{B}}_v + \Delta\overline{\boldsymbol{B}}_v(t))\boldsymbol{v}(t) \quad (21)$$

where $\overline{\boldsymbol{A}}$ and $\overline{\boldsymbol{B}}_v$ are constant matrices which come from the flight condition at Mach 0.6 and 4 572 m [9,19]:

$$\overline{\boldsymbol{A}} = \begin{bmatrix} -0.013\,4 & 48.547\,4 & -632.372\,4 & 32.075\,6 \\ -0.019\,9 & -0.120\,9 & 0.162\,8 & 0 \\ -0.002\,4 & -0.052\,6 & -0.025\,2 & 0 \\ 0 & 1 & 0.076\,8 & 0 \end{bmatrix},$$

$$\overline{\boldsymbol{B}}_v = \begin{bmatrix} 0 & 0 \\ -0.043\,1 & 0.047\,6 \\ -0.007\,6 & -0.002\,3 \\ 0 & 0 \end{bmatrix}.$$

The matrices $\Delta\overline{\boldsymbol{A}}(t), \Delta\overline{\boldsymbol{B}}_v(t)$ are chosen as

$$\begin{cases} \Delta\overline{\boldsymbol{A}}(t) = \mathrm{diag}(0, 0.2\cos t, 0.2\cos t, 0) \cdot \overline{\boldsymbol{A}} \\ \Delta\overline{\boldsymbol{B}}_v(t) = 0.3\sin 2t \cdot \overline{\boldsymbol{B}}_v \end{cases}. \quad (22)$$

The desired reference model in (2) is given as follows [9,19]:

$$\boldsymbol{A}_m = \begin{bmatrix} -0.013\,4 & 48.547\,4 & -632.372\,4 & 32.075\,6 \\ 0.538\,6 & -1.774\,6 & -23.831\,3 & -4.852\,6 \\ 0.066\,4 & 0.643\,1 & -11.247\,6 & 0.119\,2 \\ 0 & 1 & 0.076\,8 & 0 \end{bmatrix},$$

$$\boldsymbol{B}_m = \begin{bmatrix} 0 \\ 1 \\ 0 \\ 0 \end{bmatrix},$$

$$c(t) = \begin{cases} 0.4, & 10i \leqslant t \leqslant 10i+5; i = 0, 1, 2, \ldots \\ -0.4, & \text{others} \end{cases}.$$

Then the ideal control law $\boldsymbol{v}(t)$ can be designed as

$$\boldsymbol{v}(t) = -\boldsymbol{K}_1 x + \boldsymbol{K}_2 c(t) - \boldsymbol{L}(t) \tag{23}$$

where the gain matrices $\boldsymbol{K}_1$ and $\boldsymbol{K}_2$ are designed as

$$\boldsymbol{K}_1 = \begin{bmatrix} 9.9 & 63.6 & -1\,278.8 & -11.9 \\ -2.8 & 92.3 & -653.8 & 91.2 \end{bmatrix},$$

$$\boldsymbol{K}_2 = \begin{bmatrix} -4.990\,3 \\ 16.489\,8 \end{bmatrix}.$$

The expression of $\boldsymbol{L}(t)$ is

$$\boldsymbol{L}(t) = (\overline{\boldsymbol{B}}_v + \Delta\overline{\boldsymbol{B}}_v(t))^{+}[(\Delta\overline{\boldsymbol{A}}(t) - \Delta\overline{\boldsymbol{B}}_v(t)\boldsymbol{K}_1)\boldsymbol{x} + \Delta\overline{\boldsymbol{B}}_v(t)\boldsymbol{K}_2 c(t)].$$

It is easy to verify that the control law (23) can make the closed-loop system achieve the target (3) in terms of the Lyapunov theory.

Remark 4 The particular configuration of $\Delta\overline{\boldsymbol{A}}(t)$ in (22) can make the closed-loop system achieve the target (3) purely. In terms of the form of $\overline{\boldsymbol{B}}_v$, if the head or end of the diagonal of $\Delta\overline{\boldsymbol{A}}(t)$ is not zero, the tracking error $\boldsymbol{e}$ cannot meet the target (3) due to an error relating to the term $[\boldsymbol{I} - (\overline{\boldsymbol{B}}_v + \Delta\overline{\boldsymbol{B}}_v(t))(\overline{\boldsymbol{B}}_v + \Delta\overline{\boldsymbol{B}}_v(t))^{+}]$, where $\boldsymbol{I}$ denotes identity.

The mapping matrix $\boldsymbol{B}_u$ is chosen as

$$\boldsymbol{B}_u = \begin{bmatrix} 0.550\,0 & 0.676\,9 & 0 & 0.013\,88 & 0.235\,0 & 0.347\,9 & -1.748\,2 & -2.142\,9 \\ 0 & 0.006\,639 & 0.600\,0 & 0.717\,2 & -0.250\,5 & -0.358\,2 & -1.971\,2 & -2.442\,9 \end{bmatrix}.$$

The coefficient ψ in (8) is chosen as $\psi = 0.000\,25$. The parameter $\overline{\vartheta}$ in (12) is chosen as $\overline{\vartheta} = 1$. The parameters λ_g and λ_l are chosen as $\lambda_g = 2.5$ and $\lambda_l = 2.0$, respectively. The parameter η is chosen as $\eta = 2.5$. The criterion parameter χ is chosen as $\chi = 0.05$. The parameter ς in (13) is chosen as $\varsigma = 0.45$. The constraints on $\boldsymbol{n}$ are shown in Table 2.

Table 2 Constraints on $\boldsymbol{n}$

Boundary	n_1	n_2	n_3	n_4	n_5	n_6	n_7	n_8
$\underline{n}_i$	–12	–5	–12	–5	–12	–12	–10	–10
$\overline{n}_i$	12	5	12	5	12	12	10	10

According to Table 2, the number of the possible combinations of actuator states is about 2.08 billion. Although the exact optimum solution of the optimization problem (8) can be obtained by some mathematical programming solvers, certainly the solving process cannot meet the real-time requirement for the flight system. Then the proposed scheme is used to achieve it. The number of population and maximum number of iterations are chosen as 10 and 50, respectively.

First, the searching capability of the proposed scheme in one period is studied via two experiments. The initial conditions are shown in Table 3.

Table 3 Initial conditions of two experiments

Experiment number	Initial condition
1	$\boldsymbol{v}(t) = [-2.000\,0, 6.500\,0]^{\mathrm{T}}, \boldsymbol{v}(t-1) = [0,0]^{\mathrm{T}}$, $\boldsymbol{n}_p = [0,0,0,0,0,0,0,0]^{\mathrm{T}}, \vartheta = 0.5$
2	$\boldsymbol{v}(t) = [-2.500\,0, 7.000\,0]^{\mathrm{T}}, \boldsymbol{v}(t-1) =$ $[-2.500\,0, 7.000\,0]^{\mathrm{T}}$, $\boldsymbol{n}_p = [-7,-3,2,1,5,-5,-1,-1]^{\mathrm{T}}, \vartheta = 0.5$

Corresponding to the strategy (12), the initial condition of experiment 1 simulates the situation of a larger $\|\boldsymbol{v}(t)-\boldsymbol{v}(t-1)\|_2$ and the initial condition of experiment 2 simulates the situation of a smaller $\|\boldsymbol{v}(t)-\boldsymbol{v}(t-1)\|_2$. For comparison, another scheme proposed in [19] is also introduced to solve the optimization problem. To avoid contingency, each experiment is carried out 1 000 times. It should be noted that in these two experiments, the criterion parameter χ is set to $\chi = 0$ for avoiding its influence.

Firstly, the quality of the initial population is studied. The contrastive scheme is shown in Section 3.3.1 in [19]. There are 10 000 initial individuals produced by each scheme within 1 000 times runs. Their fitness values are calculated and the statistical results are shown in Table 4.

Table 4 Fitness values of initial population

Scheme	Experiment 1		Experiment 2	
	Mean	Standard	Mean	Standard
Contrastive scheme	13.047 3	7.918 7	13.028 0	7.973 2
The proposed scheme	10.345 7	4.010 3	3.640 5	3.957 0

Table 4 shows the comparison of the indices while the mean and standard deviation can indicate the quality of initial population. In terms of the results, the quality of the initial population produced by the proposed scheme outperforms that produced by the contrastive scheme. The quality of the initial individuals produced by the contrastive scheme is worse because lots of individuals go beyond the constraints (4) when they are originally created. After they are qualified via (14), their qualities cannot be ensured as planned. It also can be found that the mean of fitness values in experiment 2 is smaller than that in experiment 1. This is because in each experiment 2, according to the strategy (12), five high-quality initial individuals are inherited from $\boldsymbol{n}_p$, and other decentralized five are preferentially selected from double five alternatives created via (13). In each experiment 1, all the ten initial individuals are preferentially selected from double ten alternatives created via (13).

Secondly, the searching capability of the proposed strategies on the parameter λ and step length $\boldsymbol{\alpha}$ and the qualities of the final searched optimum solutions are studied. The proposed scheme adopts targeted $\boldsymbol{\alpha}$ and λ, and the contrastive scheme adopts fixed $\boldsymbol{\alpha}$ and λ. For eliminating the influence of the quality of initial population, both the two schemes adopt the initial population created via the proposed scheme in this paper. The fitness values of the 1 000 final searched optimum solutions are calculated and the statistical results are shown in Table 5.

Table 5 Fitness values of final searched best solutions

Scheme	Experiment 1		Experiment 2	
	Mean	Standard	Mean	Standard
Contrastive scheme	0.289 0	0.130 6	0.134 4	0.035 3
The proposed scheme	0.120 3	0.046 6	0.066 7	0.037 8

To further verify the effectiveness of the proposed scheme, a statistic ξ is added to the experiments. In the beginning of one experiment, its initial value is set to zero; if an updated individual is proved to be superior to its origin, i.e., $J(\boldsymbol{v}, \boldsymbol{n}_j^{t+1}, \boldsymbol{n}_p) < J(\boldsymbol{v}, \boldsymbol{n}_j^{t}, \boldsymbol{n}_p)$, then $\xi = \xi + 1$. It can be considered that the statistic ξ indicates the number of effective random walks. The results of ξ are illustrated in Table 6.

Table 6 Results of statistic $\boldsymbol{\xi}$

Scheme	Experiment 1		Experiment 2	
	Mean	Standard	Mean	Standard
Contrastive scheme	37.670 0	5.544 2	28.056 0	5.555 9
The proposed scheme	67.885 0	9.075 7	45.001 8	9.473 3

It can be observed that in both experiments, the numbers of effective random walks under the proposed scheme are obviously superior to those under the contrastive scheme. This can verify that the searching efficiency of the proposed scheme is higher than that of the contrastive scheme.

Next, the rationality of the selection of the parameters λ_g and λ_l is examined. In order to verify this, under the initial condition of experiment 1, another four settings of parameters λ_g and λ_l ($\lambda_g = 2.8, \lambda_l = 2.0$; $\lambda_g = 2.5, \lambda_l = 2.3$; $\lambda_g = 2.3, \lambda_l = 2.0$ and $\lambda_g = 2.5, \lambda_l = 1.8$), are put into the search and their final searched results are obtained and shown in Table 7.

Table 7 Final searching results under different settings of $\boldsymbol{\lambda_g}$ and $\boldsymbol{\lambda_l}$

Scheme	$\lambda_g = 2.5, \lambda_l = 2.0$		$\lambda_g = 2.8, \lambda_l = 2.0$		$\lambda_g = 2.5, \lambda_l = 2.3$		$\lambda_g = 2.3, \lambda_l = 2.0$		$\lambda_g = 2.5, \lambda_l = 1.8$	
	Mean	Standard	Mean	Standard	Mean	Standard	Mean	Standard	Mean	Standard
The proposed scheme	0.118 8	0.051 9	0.179 7	0.099 3	0.196 3	0.145 5	0.127 9	0.058 8	0.167 5	0.078 2

It can be observed that the best result is surely obtained under the selection of $\lambda_g = 2.5$ and $\lambda_l = 2.0$.

In terms of the above results, it can be concluded that the improvements of the proposed scheme are surely working and conducive to the acquirement of high-quality final solutions.

Second, the proposed scheme is applied to the simulative flight process (21) for verifying its performance. The fixed-step size of the simulation is set to 0.02 s and the length of the flight process is set to 20 s. The initial flight states and control inputs are set to $\boldsymbol{x}(0) = \boldsymbol{0}^{4\times1}, \boldsymbol{n}(0) = \boldsymbol{0}^{8\times1}, \boldsymbol{v}(0) = \boldsymbol{0}^{2\times1}$, $\vartheta(0) = 10$. Meanwhile, for comparison, the contrastive scheme in [19] is introduced and applied to the identical model of the flight process under identical initial conditions.

Firstly, the performances of the ideal control law (23) and the guaranteed solution $\boldsymbol{\theta}(t)$ are applied to the system. The simulation results are illustrated in Fig. 4.

It can be observed that the actual flight states can track the desired reference model exactly under the ideal control law (23). It can also be observed that the tracking performance under the guaranteed solution $\boldsymbol{\theta}(t)$ is stable but inferior. Therefore, the guaranteed solution $\boldsymbol{\theta}(t)$ can be utilized to ensure the flight stability when the quality of the searched solution obtained via the metaheuristic algorithm is poor but a further control allocation scheme is necessary for ICE aircraft to improve the tracking performance.

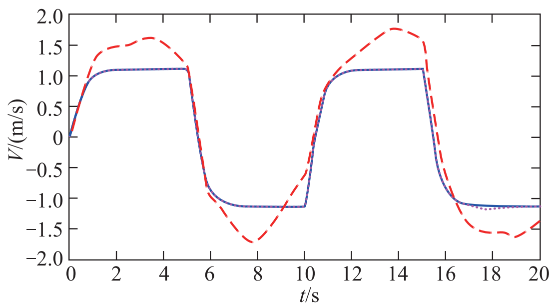

(a) Velocity

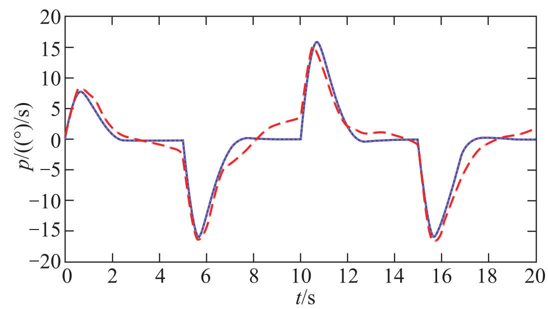

(b) Roll rate

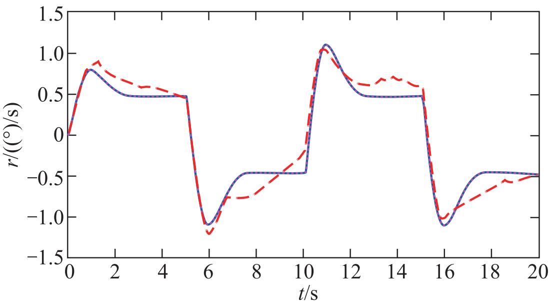

(c) Yaw rate

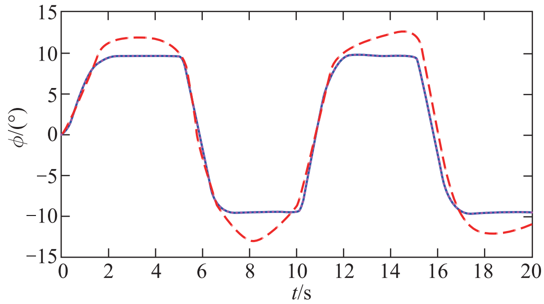

(d) Roll angle

—— : Reference; ······ : Ideal control input $\boldsymbol{v}(t)$;
– – : Guaranteed solution $\boldsymbol{\theta}(t)$.

Fig. 4 State responses under ideal control law and guaranteed solution

Secondly, the proposed control allocation scheme and the contrastive scheme are applied to the flight system. The simulation results under the two schemes are illustrated in Fig. 5 – Fig. 7 and Table 8 and Table 9.

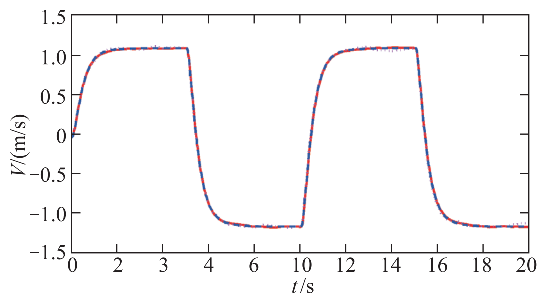

(a) Velocity

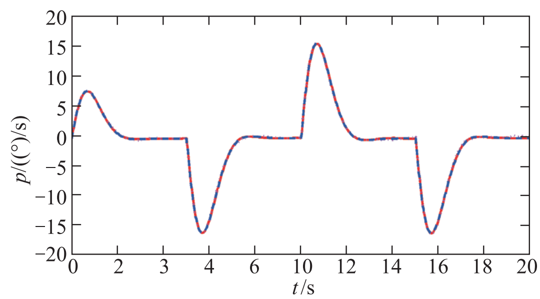

(b) Roll rate

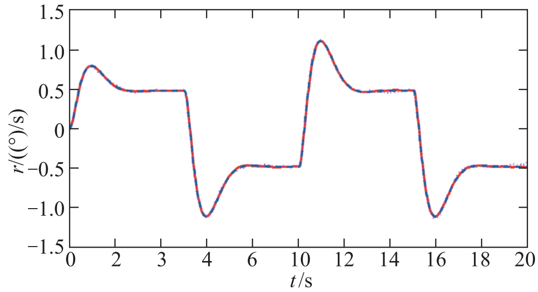

(c) Yaw rate

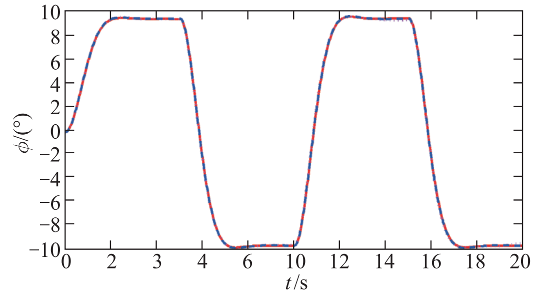

(d) Roll angle

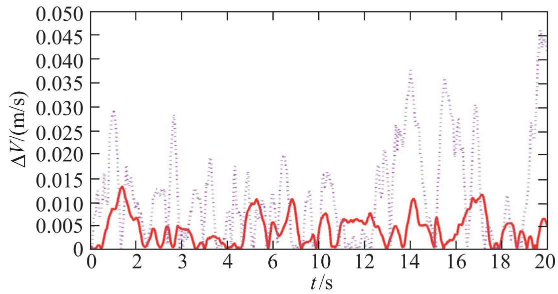

(e) Velocity tracking error

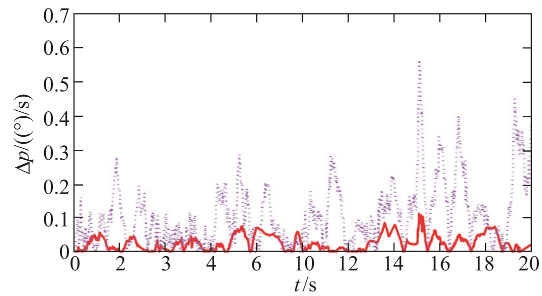

(f) Roll rate tracking error

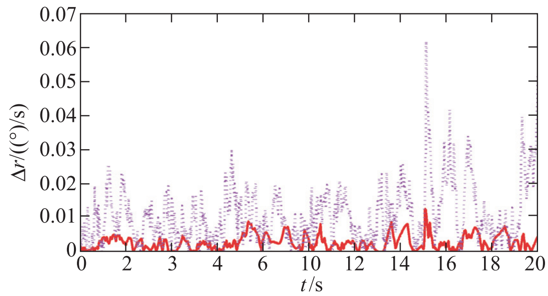

(g) Yaw rate tracking error

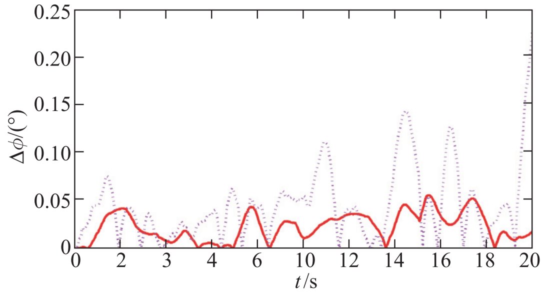

(h) Roll angle tracking error

: The proposed scheme; : Contrastive scheme; : Reference.

Fig. 5 State responses and tracking errors under the proposed scheme and the contrastive scheme

Fig. 5 illustrates the state responses and tracking errors of the closed-loop system. In Fig. 5(b), the labels of the y-axis denote the absolute values of elements of the tracking error $\boldsymbol{e}$. To avoid contingency, 1 000 times simulative flight processes under identical initial conditions are carried out and the averages of the accumulated tracking errors of all the 1 000 sample points in one flight process are counted. The statistical results are shown in Table 8.

Table 8 Accumulated errors per flight process

Scheme	Accumulated ΔV per flight process/ (m/s)	Accumulated Δp per flight process/ ((°)/s)	Accumulated Δr per flight process/ ((°)/s)	Accumulated $\Delta\phi$ per flight process/ (°)
Contrastive scheme	11.470 3	109.914 5	10.815 5	45.668 4
The proposed scheme	4.291 4	28.506 9	2.775 6	22.899 4

From Fig. 5 and Table 8, it can be observed that the tracking performance under the proposed scheme is superior to that under the contrastive scheme. Considering the previous results from Table 5 – Table 7, this result is normal due to the stronger searching capability the proposed scheme has.

Fig. 6 illustrates the commands of actuators under the proposed and contrastive schemes. It can be obviously observed that the changes of the states of actuators under the contrastive scheme are more drastic than those under the proposed scheme. To avoid contingency, the averages of number of state switches of eight actuator groups from the above-mentioned 1 000 times simulative flight processes are counted. The statistical results are shown in Table 9.

It can be observed that the results are similar to those in Fig. 6. This is because the contrastive scheme does not utilize former searched results to conduct the population initialization in the new searching process, i.e., its searching process is independent in each sample point. For the proposed scheme, the strategy on population initialization decreases the probability of drastic change when the last searching result is superior. From Fig. 5(a) – Fig. 5(d) and Fig. 6(a), it can be noticed that the changes of the actuator states are relatively smooth at those sample points which are far from the switching points of $c(t)$ (5 s, 10 s, 15 s). This is because the indices ϑ and $\|\boldsymbol{v}(t)-\boldsymbol{v}(t-1)\|_2$ are usually smaller at those smooth intervals. Thus, the situation of their initial individuals is similar to the above-mentioned experiment 2 in Table 4, i.e., a part of the initial individuals are inherited from the last $\boldsymbol{n}_p$ with high qualities.

Table 9 Average of number of actuator state switches per sample point

Scheme	Number of state switches per sample point							
	n_1	n_2	n_3	n_4	n_5	n_6	n_7	n_8
Contrastive scheme	7.663	3.844	7.595	4.003	7.809	7.045	6.986	5.763
The proposed scheme	1.210	0.757	1.223	0.770	1.416	1.264	1.043	0.846

Fig. 7 illustrates the comparison between the ideal control input $\boldsymbol{v}(t)$ and actual actuator control input $\boldsymbol{B}_u\boldsymbol{n}(t)$ from (5) under the proposed control allocation scheme. In Fig. 7, the labels of the y-axis $\boldsymbol{v}(1)$ and $\boldsymbol{v}(2)$ denote the first and last elements of the two-dimensional column vector $\boldsymbol{v}(t)$, respectively. This result can further show the effectiveness of the proposed scheme. Moreover, it can be observed that the control input $\boldsymbol{v}(2)$ at 15 s is larger than that at 5 s under the same $c(t)$. This is because the disturbance $\Delta\overline{\boldsymbol{B}}_v(15)$ is larger than $\Delta\overline{\boldsymbol{B}}_v(5)$.

In addition, the average of the statistical elapsed time of one simulative process under the proposed scheme is about 3.178 s with the setting that $\chi=0$ and an Intel Core i7-4 790 CPU @3.60 GHz. That is, one single searching process at one sample point takes up about 6.356 ms on average. Meanwhile, the statistical maximum of computational time at one sample point is 6.562 ms. This computational speed is acceptable to most flight vehicle control systems.

In terms of the characteristic of the metaheuristic algorithm, although the qualities of solutions obtained via the proposed scheme are uncertain in limit time in theory, the condition $\overline{J}(\boldsymbol{\theta})<\overline{J}(\boldsymbol{n})$ for replacing $\boldsymbol{n}$ with $\boldsymbol{\theta}$ mentioned is rarely reached due to the inferior $\overline{J}(\boldsymbol{\theta})$ which can be observed from Fig. 4. To simulate the uncertainty and further verify the effectiveness of the proposed guaranteed strategy, an artificial setting that uses the guaranteed solution $\boldsymbol{\theta}$ as the actuator control command without searching every 0.1 s is put into the simulative flight process. The simulation result is illustrated in Fig. 8.

It can be observed that the closed-loop system is stable and the tracking performance is between the result under the proposed scheme from Fig. 5(e) – Fig. 5(h) and the result under pure guaranteed solution from Fig. 4. Therefore, the effectiveness of the proposed guaranteed strategy is further verified.

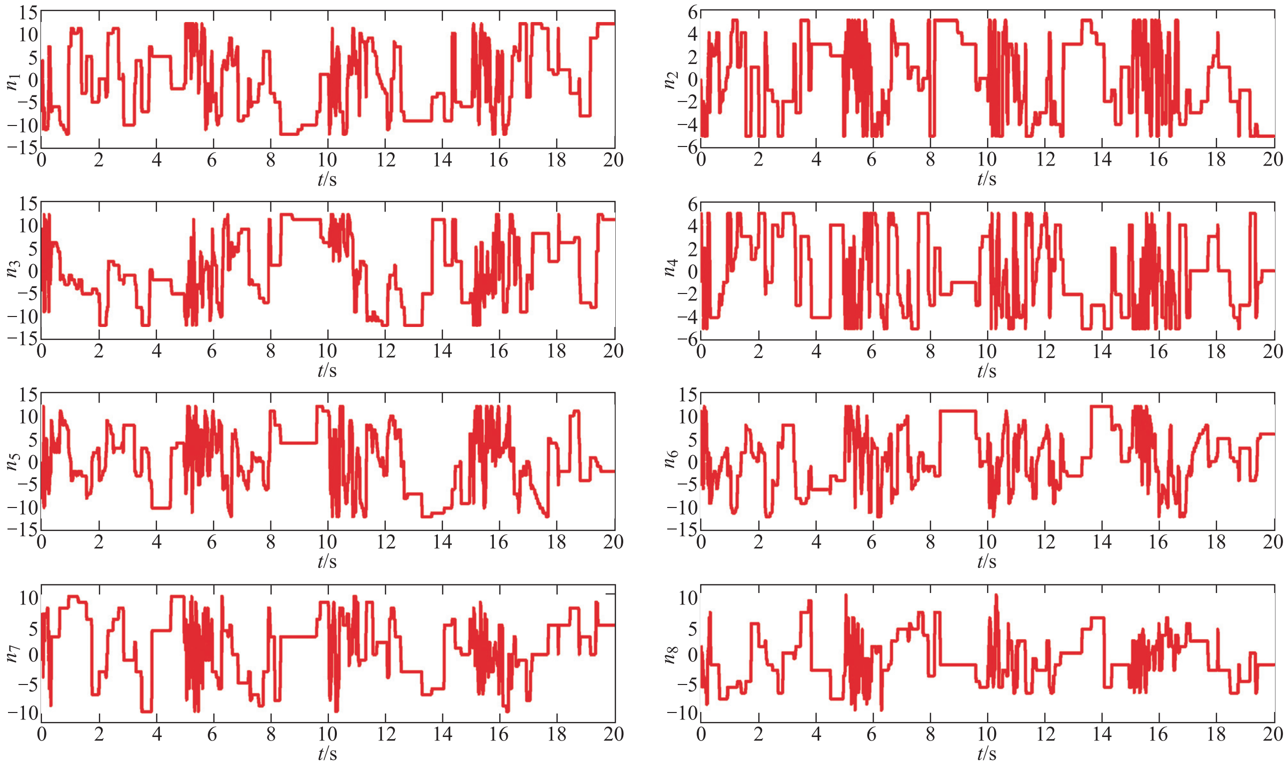

(a) The proposed scheme

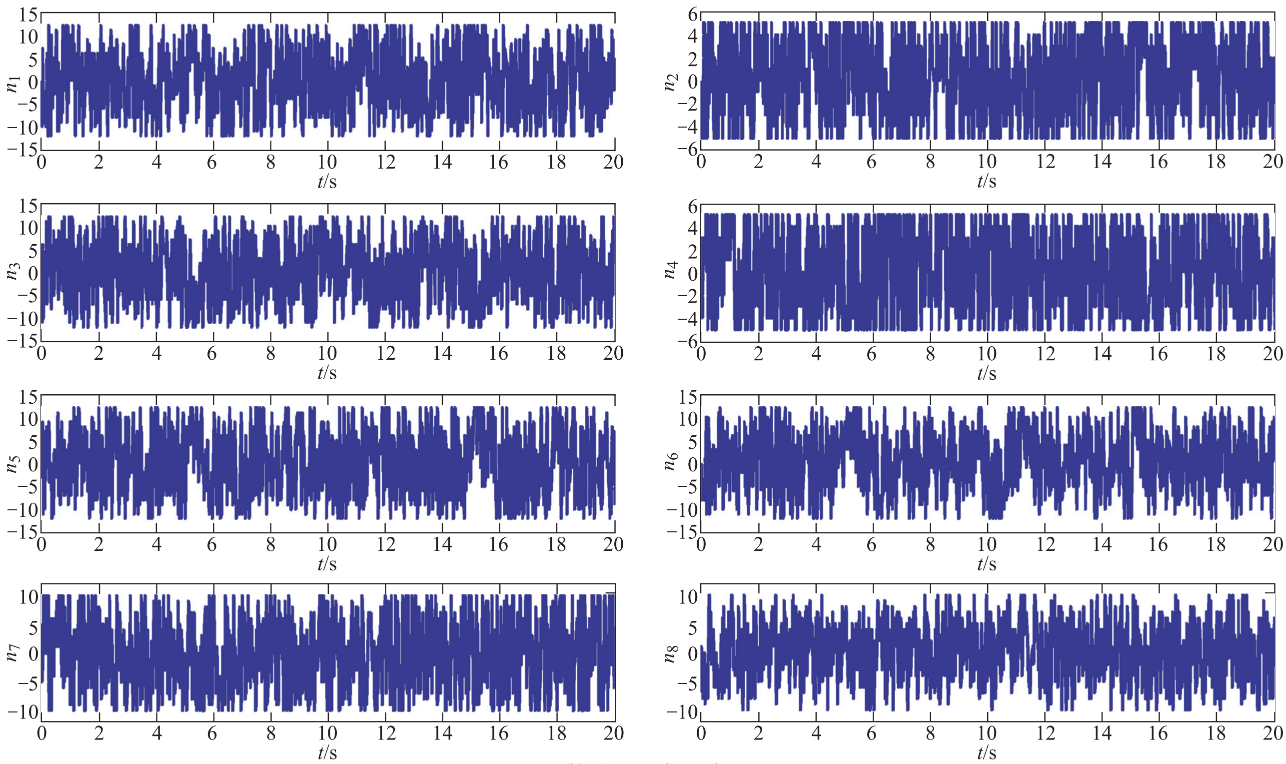

(b) Contrastive scheme

Fig. 6 Actuator control command

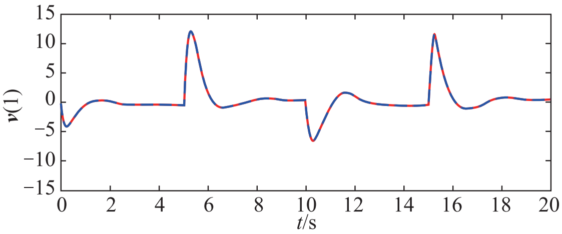

(a) Vector element $\boldsymbol{v}(1)$

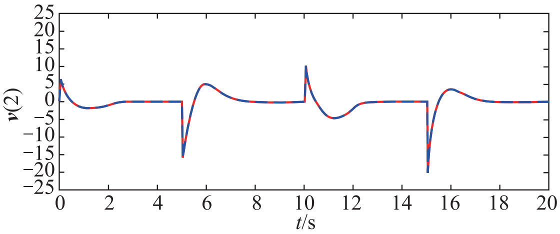

(b) Vector element $\boldsymbol{v}(2)$

: Actual control input $\boldsymbol{B}_u\boldsymbol{n}(t)$; : Ideal control law $\boldsymbol{v}(t)$.

Fig. 7 Comparison between ideal control input and actuator control input under the proposed scheme

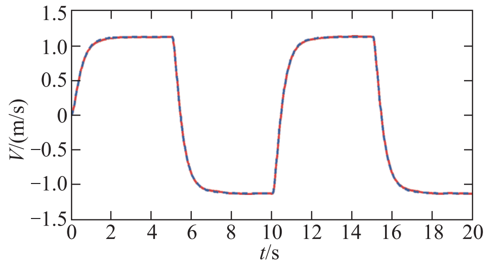

(a) Velocity

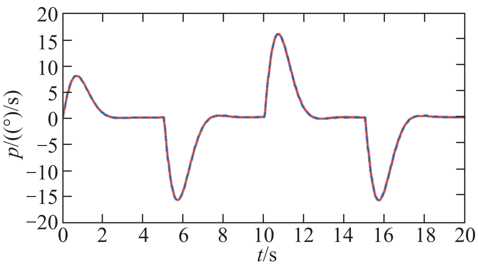

(b) Roll rate

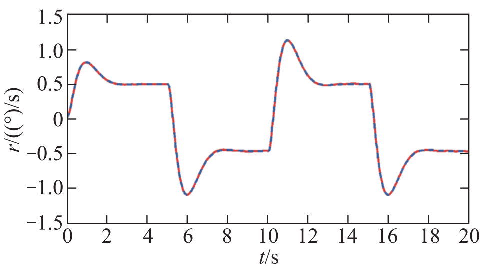

(c) Yaw rate

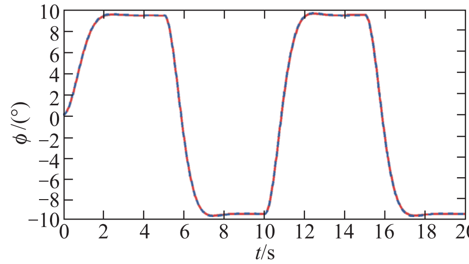

(d) Roll angle

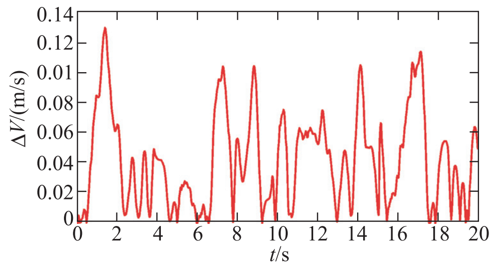

(e) Velocity tracking error

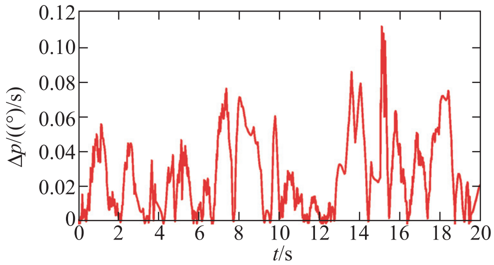

(f) Roll rate tracking error

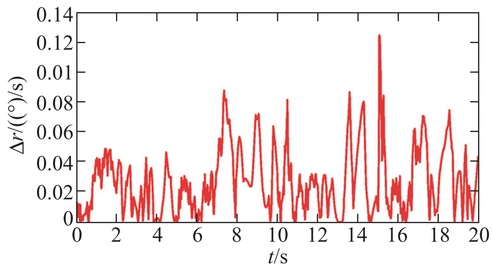

(g) Yaw rate tracking error

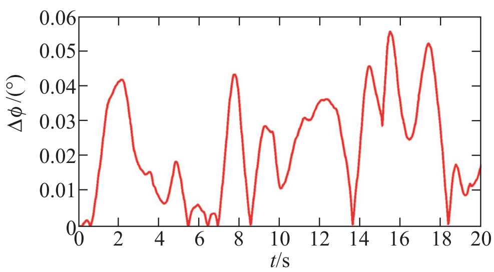

(h) Roll angle tracking error

: The proposed scheme with discontinuous $\boldsymbol{\theta}$;

: Reference.

Fig. 8 State responses and tracking errors under the proposed scheme with discontinuous $\boldsymbol{\theta}$

Remark 5 According to the stability analysis and simulation results, it can be known that the tracking error $\boldsymbol{e}$ can be ensured bounded in theory, and due to the guaranteed solution $\boldsymbol{\theta}$, the flight states of ICE aircraft can still keep stable even if the searching processes are inefficient. Moreover, it is verified in simulation that the computing time of the proposed method can be acceptable to most flight control systems. Therefore, it can be concluded that the utility of the approach to ICE aircraft is better.

5. Conclusions and future work

A control allocation scheme for tracking control of ICE aircraft is proposed. In this scheme, two desired objectives, tracking accuracy and energy consumption of actuators, are considered and represented as an optimization problem. Following that, the Lévy flight is introduced for exploring the optimum solution. Meanwhile, some improvements in step length, population initialization and other heuristic strategies are proposed for searching efficiency. To prevent possible low-quality solutions obtained via the proposed scheme, a guaranteed strategy is proposed for ensuring flight stability. To verify the effectiveness of the proposed scheme, a time-varying ICE aircraft model is introduced and some contrastive simulations are carried out. The simulation results show that the proposed control allocation scheme can achieve superior tracking performance with a low-level wear and tear of actuators and the proposed improvements are effective. The study of this paper indicates that for an optimization problem with requirement of real-time, metaheuristic algorithms are especially noteworthy tools to tackle it.

Future studies are planned to be classified in two directions. One is to find and summarize the connection between the flight dynamics and the actions of actuators thoroughly for supplying heuristic searching directions. The other direction is to improve the search efficiency from the metaheuristic algorithm itself, including designing appropriate computing strategies on the parameters of the algorithm, cancelling some unnecessary comparison operations, and so on.

References

[1] JOHANSEN T A, FOSSEN T I. Control allocation — a survey. Automatica, 2013, 49(5): 1087 – 1103.

[2] FROMHERZ M P J, JACKSON W B. Force allocation in a large-scale distributed active surface. IEEE Trans. on Control Systems Technology, 2003, 11(5): 641 – 655.

[3] LIU C S, ZHANG S J. Novel robust control framework for morphing aircraft. Journal of Systems Engineering and Electronics, 2013, 24(2): 281 – 287.

[4] ZHI J H, CHEN Y, DONG X M, et al. Robust adaptive FTC allocation for overactuated systems with uncertainties and unknown actuator non-linearity. IET Control Theory Application, 2018, 12(2): 273 – 281.

[5] YU G X, LI H F. Hierarchical structured robust adaptive attitude controller design for reusable launch vehicles. Journal of Systems Engineering and Electronics, 2015, 26(4): 813 – 825.

[6] RANEY D L, MONTGOMERY R C, GREEN L L, et al. Flight control using distributed shape-change effector arrays. Proc. of the 41st AIAA/ASME/ASCE/AHS/ASC Structures, Structural Dynamics, and Materials Conference & Exhibit, 2000: AIAA 2000-1560.

[7] TAO G, TANG X, CHEN S H, et al. Adaptive failure compensation of two-state aircraft morphing actuators. IEEE Trans. on Control Systems Technology, 2006, 14(1): 157 – 164.

[8] LIU C S, JIANG B. Fault-tolerant control allocation for over-actuated discrete-time systems. Journal of the Franklin Institute, 2015, 352(6): 2297 – 2313.

[9] ATAEI-ESFAHANI A, WANG Q. Robust failure compensation for a morphing aircraft model using a probabilistic approach. IEEE Trans. on Control Systems Technology, 2007, 15(2): 324 – 331.

[10] LIU C S, LI C, HE Z. Adaptive control of a morphing aircraft through updating the number of actuators. Proc. of the AIAA Guidance, Navigation, and Control Conference, 2012: AIAA 2012-4446.

[11] KOKEN P, RAGHAVAN V A, YOON S W. A genetic algorithm based heuristic for dynamic lot sizing problem with returns and hybrid products. Computers & Industrial Engineering, 2018, 119: 453 – 464.

[12] QIU Y Z, WANG L, XU X L, et al. A variable neighborhood search heuristic algorithm for production routing problems. Applied Soft Computing, 2018, 66: 311 – 318.

[13] DAVIDSON P P, BLUM C, LOZANO J A. The weighted independent domination problem: integer linear programming models and metaheuristic approaches. European Journal of Operational Research, 2018, 265(3): 860 – 871.

[14] ATOUI W S, AJIB W, BOUKADOUM M. Offline and online scheduling algorithms for energy harvesting RSUs in VANETs. IEEE Trans. on Vehicular Technology, 2018, 67(7): 6370 – 6382.

[15] WOO Y B, KIM B S. Matheuristic approaches for parallel machine scheduling problem with time-dependent deterioration and multiple rate-modifying activities. Computers and Operations Research, 2018, 95: 97 – 112.

[16] SHENG L, KAPANIA R K. Comparison of genetic algorithms and heuristic integer programming on the optimization of piezoelectric actuator locations. Proc. of the 11th AIAA/ISSMO Multidisciplinary Analysis and Optimization Conference, 2006. DOI:10.2514/6.2006-6909.

[17] CZIBULA O G, GU H Y, ZINDER Y. Lagrangian relaxation versus genetic algorithm based metaheuristic for a large partitioning problem. Theoretical Computer Science, 2018, 718: 24 – 36.

[18] LU Y, DONG C Y, WANG Q. Control allocation for aircraft with input constraints based on improved cuckoo search algorithm. Defence Technology, 2017, 13(1): 1 – 5.

[19] DONG C Y, LU Y, WANG Q. Tracking control based on control allocation with an innovative control effector aircraft application. Mathematical Problems in Engineering, 2016: 5037678.

[20] QIN Q, FENG Y W, LI F. Structural reliability analysis using enhanced cuckoo search algorithm and artificial neural network. Journal of Systems Engineering and Electronics, 2018, 29(6): 1317 – 1326.

[21] PARE S, KUMAR A, BAJAJ V, et al. An efficient method for multilevel color image thresholding using cuckoo search algorithm based on minimum cross entropy. Applied Soft Computing, 2017, 61: 570 – 592.

[22] REYNOLDS A M, SMITH A D, MENZEL R, et al. Displaced honey bees perform optimal scale-free search flights. Ecology, 2007, 88 (8): 1955 – 1961.
[23] SHLESINGER M F. Mathematical physics: search research. Nature, 2006, 443(7109): 281 – 282.
[24] YANG X S, DEB S. Cuckoo search: recent advances and applications. Neural Computing and Applications, 2014, 24(1): 169 – 174.
[25] LIU X Y, FU M L. Cuckoo search algorithm based on frog leaping local search and chaos theory. Applied Mathematics and Computation, 2015, 266: 1083 – 1092.
[26] HE J, YAO X. Towards an analytic framework for analysing the computation time of evolutionary algorithms. Artificial Intelligence, 2003, 145(1/2): 59 – 97.

Biographies

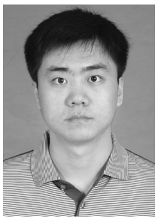

LU Yao was born in 1987. He received his Ph.D. degree in flight vehicle design from Beihang University in 2017. He is currently an engineer in Beijing Aerospace Automatic Control Institute. His research interests include nonlinear control and intelligence control.
E-mail: luyaosacred@126.com

SUN You was born in 1979. He received his M.S. degree in guidance, navigation and control from Beijing Institute of Technology in 2004. He is currently a professor of engineering in Beijing Aerospace Automatic Control Institute. His research interests include missile guidance and control, guided projectile, and fault detection.
E-mail: sunyou1979@126.com

LIU Xiaodong was born in 1987. He received his Ph.D. degree in guidance, navigation and control from Beihang University in 2013. He is currently an engineer in Beijing Aerospace Automatic Control Institute. His research interests include hypersonic flight control, integrated guidance and control and intelligence control.
E-mail: k.start@163.com

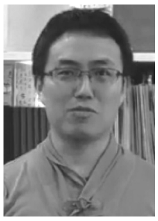

GAO Bo was born in 1986. He received his M.S. degree in guidance, navigation and control from Beihang University in 2011. He is currently an engineer in Beijing Aerospace Automatic Control Institute. His research interests include robotic control and fuzzy control.
E-mail: gaobo1986_buaa@126.com